# Optimal Conflict Resolution for Air Traffic Control

Antonio Bicchi Lucia Pallottino
Dept. Electrical Systems and Automation
&
The Interdept. Research Center "Enrico Piaggio"
University of Pisa
via Diotisalvi, 2, 56100 Pisa, Italy.

## Abstract

*In this paper, we consider optimal resolution of air traffic conflicts. Aircraft are assumed to cruise within a given altitude layer, and are modeled as a kinematic system with velocity constraints and curvature bounds. Aircraft can not get closer to each other than a predefined safety distance. For such system of multiple aircraft, we consider the problem of planning optimal paths among given way-points. Necessary conditions for optimality of solutions are derived, and used to devise a parameterization of possible trajectories that turns into efficient numerical solutions to the problem. Simulation results for a realistic aircraft conflict scenario are provided.*

## 1 Introduction

Aircraft coordination in increasingly crowded airspace is becoming a major concern for air traffic management authorities in the U.S., Japan, and Europe [1, 2]. Conventional management schemes are being replaced by extensively computer–integrated Air Traffic Management Systems (ATMS) to maintain safety levels and increase throughput of congested airways. On the other hand, today's aircraft instrumentation and communications allow increasingly complex decisions to be taken on-board, thus enabling a progressive move towards decentralized control scenarios often referred to as free–flight ATMS [3, 4].

Our work is aimed at providing efficient algorithms for conflict resolution and strategies which are inherently safe and minimize fuel consumption, to address pollution as well as economic concerns. In this paper, we apply optimal control and game theory (in particular team theory), to a kinematic model of airtraffic. In particular, we refer to general decentralized ATM architectures such as that of [5]. Each aircraft in the system has an initial flight plan which has been designed by this central authority, and is encoded as a sequence of way points from origin to destination. The planning and control hierarchy on board each aircraft uses this sequence of way points as input, and generates a full state trajectory for the aircraft. However, unmodeled "disturbances" in the air traffic system (such as bad weather, wind, mechanical problems with a single aircraft) can force the aircraft to deviate from their original flight paths. In such situations, aircraft should be able to resolve "local" deviations, such as within a sector away from a TRACON.

Specifically, we will address the problem of planning motions of a system of multiple aircraft whose dynamics are described by the point–mass model [6, 7]. Aircraft conflicts are modelled as collisions between the "conflict envelopes" that surround each aircraft. We make the central assumption that conflicts are to be solved while aircraft cruise within a fixed altitude layer. Aircraft can thus be modeled in a purely kinematic fashion, as points in a plane with an associated fore axis and conflict envelope radius. The task of each vehicle is to reach a given goal configuration from a given start configuration. Optimal solutions in the sense of minimizing total path length and total time will be considered.

Another important assumption we make is that all interacting aircraft cooperate towards optimization of a common goal, as agents in the same team. Such cooperative game approach is to be contrasted with the antagonistic approach developed by [8], which results in single–aircraft strategies that are safe against worst–case maneuvers of all other potentially conflicting vehicles.

In this paper, we will discuss necessary conditions for optimality of conflict resolution schemes, and will derive from these conditions algorithms that numerically determine such solutions.

## 2 Modeling

The point–mass aircraft model is a widely accepted description of dynamical effects encountered in civil aviation [9]. It consists of six equations, which, disregarding earth rotation and curvature, are

$$\begin{aligned}
\dot{x} &= V\cos\gamma\cos\chi; && (1)\\
\dot{y} &= V\cos\gamma\sin\chi; && (2)\\
\dot{h} &= V\sin\gamma; && (3)\\
\dot{\gamma} &= \frac{g}{V}(n\cos\varphi-\cos\gamma); && (4)\\
\dot{\chi} &= \frac{g}{V}\frac{n\sin\varphi}{\cos\gamma}; && (5)\\
\dot{V} &= \frac{T-D}{m}-g\sin\gamma. && (6)
\end{aligned}$$

Here $x, y, h$ denote the components of the position of the center of gravity (c.g.) of the aircraft in a ground–based reference frame, and are usually referred to as down–range (or longitude), cross-range (or latitude), and altitude, respectively. Angles are also defined with respect to the same

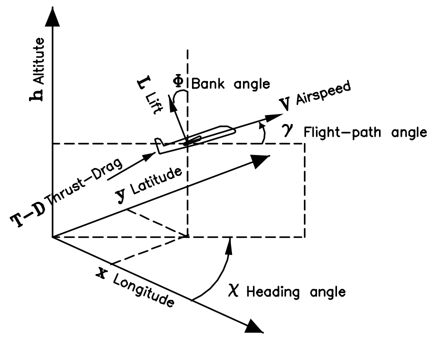


Figure 1: Aircraft coordinate system

frame: $\varphi$ is the bank angle, $\chi$ is the heading angle, and $\gamma$ is the flight-path angle (see fig.1). The ground speed velocity, $V$, is assumed to be equal to airspeed. where $T$ is the engine thrust, $D$ is the aerodynamic drag, $m$ the aircraft mass, $g$ the gravity acceleration. Notice that the thrust depends on the altitude $h$, Mach number $M$; also, it is assumed that the drag is a known function of $h$, $M$, and of the aerodynamic lift $L$. The bank angle $\varphi$, the engine thrust $T$, and the load factor $n$ are the control variables for the aircraft. The bank angle is commanded combining rudder and ailerons trims; the thrust is commanded by the engine throttle, and the load factor by elevators ($n = \frac{L}{gm}$). Using suitable nonlinear feedback of states (described in detail e.g. in [10] or [9]), the point–mass model can be linearized to Brunovsky's canonical form, i.e.

$$\dddot{x} = U_x;\ \dddot{y} = U_y;\ \ddot{h} = U_h, \qquad (7)$$

and the ensuing linear system can be easily controlled along planned trajectories $x_{des}(t), y_{des}(t), h_{des}(t)$ by adopting robust linear control techniques.

In air traffic conflict resolution, a crucial consideration is the separation constraint, imposing that the so–called conflict envelopes of all aircraft do not overlap during flight. The current definition of conflict ([11]) of two aircraft involves that their altitude differs by less than $2000$ ft. or that they get closer, in an horizontal plane, than $5$ n. miles. The constraint can be visualized by considering for each aircraft a disk $2000$ft. high and with a $2.5$n. miles radius, centered in the aircraft representative point (e.g., the c.g.): in this case, the separation constraint imposes that the disks do not overlap during flight.

First, we consider air traffic problems that possess an altitude–layered structure, in which the airspace is subdivided in horizontal layers of depth and no conflict can happen between aircraft of different layers ([12]). Conflicts need only to be resolved among aircraft flying within the same layer, and only the distance between projections of the aircraft c.g.'s on a horizontal plane need to be considered. As a consequence, to all practical purposes in the problem at hand, we may assume that longitudinal dynamics are regulated independently from the conflict resolution problem, and disregard altitude variations in the model.

A simplified planar aircraft model can then be adopted as

$$\dot{x} = u\cos\chi; \qquad (8)$$
$$\dot{y} = u\sin\chi; \qquad (9)$$
$$\dot{\chi} = \omega; \qquad (10)$$

where $u \stackrel{def}{=} V\cos\gamma$ is the horizontal velocity, and $\omega \stackrel{def}{=} \frac{L\sin\varphi}{m}\frac{1}{u}$. Furthermore, we assume that forward dynamics (6) can be effectively controlled by the autopilot so as to track a given reference $\hat{V}(t)\cos\hat{\gamma}(t) = \hat{u}(t)$, with negligible errors, provided that the reference airspeed belongs to a given interval and is sufficiently smooth. We will henceforth regard $u$ and $\omega$ as control inputs to the kinematic model (8) through (10). Bounds on the airspeed $V_{min} \le V \le V_{max}$, and on the flight–path angle, $|\gamma| \le \gamma_{max}$, reflect in bounds on the new inputs as

$$V_{min}\cos\gamma_{max} \stackrel{def}{=} U_{min} \le u \le U_{max} \stackrel{def}{=} V_{max} \qquad (11)$$

The other input to the kinematic planar aircraft model is $\omega$, whose physical dimensions are those of an angular velocity, and will be termed *yaw rate*. Constraints on the yaw rate result from constraints on the bank angle $|\varphi| \le \varphi_{max}$ and on the aerodynamic lift, which is proportional to the square of airspeed:

$$|L| \le \beta_L V^2 \qquad (12)$$

Accordingly, a bound on the yaw rate is obtained as

$$|\omega| \le \frac{u}{R}, \qquad (13)$$

where $R \stackrel{def}{=} \frac{m\cos^2\gamma_{max}}{\beta_L \sin|\varphi_{max}|}$. The constant $R$ has the dimensions of a length, and actually, in the kinematic model (8) — (10), (13) defines the minimum curvature radius that planar trajectories of the aircraft may achieve (the bound is actually achieved in planar cruise, $\gamma = 0$).

## 2.1 Optimization Problem Statement

According to previous discussion, consider $N$ vehicles in the plane, whose individual configuration is described by $\xi_i = (x_i, y_i, \chi_i) \in \mathbf{R}\times\mathbf{R}\times S^1$. Each vehicle is assigned two waypoint configurations, $\xi_{i,s}$ and $\xi_{i,g}$, respectively. The initial waypoint time is assigned and denoted by $T_i^s$. Assume vehicles are ordered such that $T_1^s \le T_2^s \le \cdots \le T_N^s$. We denote by $T_i^g$ the time at which the $i$–th vehicle reaches its goal, and let $T_i \stackrel{def}{=} T_i^g - T_i^s$. Motions of the $i$–th vehicle before $T_i^s$ and after $T_i^g$ are not of interest. The $i$–th vehicle motion is described by the control system $\dot{\xi}_i = f_i(\xi_i, u_i, \omega_i)$, with

$$f_i(\xi_i, u_i, \omega_i) = \begin{pmatrix} u_i\cos\chi_i \\ u_i\sin\chi_i \\ \omega_i \end{pmatrix}. \qquad (14)$$

All vehicles are subject to the following constraints:

**i)** the linear velocity is bounded: $U_{i,min} \le u_i \le U_{i,max}$;

**ii)** the path curvature is bounded: $|\omega_i| \leq \Omega_i$, where $\Omega_i = \frac{|u_i|}{R_i}$ and $R_i > 0$ denotes the minimum curvature radius of trajectories for the $i$–th vehicle;

**iii)** the distance between two vehicles must remain larger than, or equal to, a given separation limit: $D_{ij}(t) = (x_j(t) - x_i(t))^2 + (y_j(t) - y_i(t))^2 - d_{ij}^2 \geq 0$, at all times $t$ ($d_{ii} = 0, i = 1, \ldots, N$).

The length of the planar path joining the waypoints for the $i$–th vehicle is

$$L_i = \int_{T_i^s}^{T_i^g} \sqrt{\dot{x}_i^2 + \dot{y}_i^2} dt = \int_{T_i^s}^{T_i^g} u_i dt \qquad (15)$$

Consider the optimal conflict resolution problem for multiple vehicles defined as:

$$\begin{cases} \min \sum_{i=1}^N J_i \\ \dot{\xi}_i = f_i(\xi_i, u_i, \omega_i) \;\; i = 1, \ldots, N \\ U_{i,min} \leq u_i \leq U_{i,max} \;\; i = 1, \ldots, N \\ |\omega_i| \leq \frac{|u_i|}{R_i} \;\; i = 1, \ldots, N \\ D_{ij}(t) \geq 0, \;\; \forall t, \; i, j = 1, \ldots, N \\ \xi_i(T_i^s) = \xi_{i,s}, \quad \xi_i(T_i^g) = \xi_{i,g}. \end{cases} \qquad (16)$$

where $J_i = L_i$ for shortest total path problems, and $J_i = T_i$ for minimum total time problems.

In this paper, we restrict to the case that the aircraft velocity $u_i$ are constant. In this hypothesis, the two problems are equivalent, and we will henceforth use the minimum total time formulation.

If separation constraints are disregarded, the minimum total length problem is clearly equivalent to $N$ independent minimum length problems under the above constraints, i.e. to $N$ classical Dubins' problems, for which solutions are well known in the literature ([13, 14, 15]). It should be noted that computation of the Dubins solution for any two given configurations is computationally very efficient.

The shortest total path problem has a straightforward solution in terms of the $N$ independent Dubins' solutions, even when taking separation constraints into account, provided that there exists an associated velocity profile satisfying (11) which guarantees separation. We will henceforth consider the minimum total time problem.

### 2.2 Formulation as an Optimal Control Problem

Notice that the cost for the total time problem, $J = \sum_{i=1}^N T_i = \sum_{i=1}^N \int_{T_i^s}^{T_i^g} dt$, is not in the standard Bolza form. In order to use powerful results from optimal control theory, we rewrite the problem as follows. Let $h(t)$ denote the Heavyside function, i.e. $h(t) = 0$ for $t < 0$ and $h(t) = 1$ for $t \geq 0$ and define the window function $w_i(t) = h(t - T_i^s) - h(t - T_i^g)$. Then the minimum total time cost is written as $J = \int_0^\infty \sum_{i=1}^N w_i(t) dt$.

Using the notation $\mathrm{col}_{i=1}^N (v_i) = \left[v_1^T, \ldots, v_N^T\right]^T$, define the aggregated state $\xi = \mathrm{col}_{i=1}^N (\xi_i)$, controls $u = \mathrm{col}_{i=1}^N (u_i)$ and $\omega = \mathrm{col}_{i=1}^N (\omega_i)$, and define the admissible control sets $U$ and $\Omega$ accordingly. Also define the separation vector $D = [D_{12}, \cdots, D_{1N}, D_{23}, \cdots, D_{N-1,N}]$, and define the vector field $f(\xi, u, \omega) = \mathrm{col}_{i=1}^N (f_i w_i)$. Finally introduce matrices $\Gamma_i = \mathrm{col}_{j=1}^N (\sigma_{ij} [1\ 1\ 1]^T)$, with $\sigma_{ij} = 1$ if $i = j$, else $\sigma_{ij} = 0$, and functions $\gamma_i(\xi(t), \bar{\xi}) = \Gamma_i \left(\xi(t) - \bar{\xi}\right)$. Our optimal control problem is then formulated as

**Problem 1.** *Minimize $J$ subject to $\dot{\xi} = f(\xi, u, \omega)$, $\omega \in \Omega$, $D \geq 0$, and to the two sets of N interior–point constraints*

$$\begin{array}{l} \gamma_i(\xi(t), \xi_i^s) = 0, \;\; t = T_i^s \\ \gamma_i(\xi(t), \xi_i^g) = 0, \;\; t = T_i^g (\text{unspecified}) \end{array}$$

# 3 Necessary conditions

Necessary conditions for problem 1 can be studied by adjoining the cost function with the constraints multiplied by unspecified Lagrange covectors. Omitting to write explicitly the extents of iterative operations when extending from 1 to N, let

$$\begin{array}{l} \hat{J} = \sum_i \pi_i^s \gamma_i(\xi(T_i^s) - \xi_i^s) + \sum_i \pi_i^g \gamma_i(\xi(T_i^g) - \xi_i^g) \\ \quad + \int_0^\infty \sum_i w_i + \lambda^T(\dot{\xi} - f) + \nu^T D \, dt, \end{array} \qquad (17)$$

with $\lambda$ and $\nu$ costates of suitable dimension, and with $\nu_i = 0$ if $D_i > 0$, $\nu_i \geq 0$ if $D_i = 0$. Let the Hamiltonian be defined as $H = \sum_i w_i + \lambda^T f + \nu^T D$. Substituting previous equation in (17), integrating by parts, and computing the variation of the cost, one gets:

$$\begin{array}{rl} \delta\hat{J} = & \sum_i \left[\lambda^T(T_i^{s-}) - \lambda^T(T_i^{s+}) + \pi_i^s \frac{\partial \gamma_i}{\partial \xi(T_i^s)}\right] d\xi(T_i^s) \\ & + \sum_i \left[\lambda^T(T_i^{g-}) - \lambda^T(T_i^{g+}) + \pi_i^g \frac{\partial \gamma_i}{\partial \xi(T_i^g)}\right] d\xi(T_i^g) \\ & + \sum_i \left[H(T_i^{g-}) - H(T_i^{g+}) + \pi_i^g \frac{\partial \gamma_i}{\partial T_i^g}\right] dT_i^g \\ & + \int_0^\infty \left[\left(\dot{\lambda}^T + \frac{\partial H}{\partial \xi}\right) \delta\xi + \frac{\partial H}{\partial \omega} \delta\omega\right] dt \end{array} \qquad (18)$$

(recall that $dT_i^s \equiv 0$). Therefore, we have the following necessary conditions for an extremal solution:

$$\lambda_i(T_i^{s-}) = \lambda_i(T_i^{s+}) + \Gamma_i^T \pi_i^s \qquad (19)$$

$$\lambda_i(T_i^{g-}) = \lambda_i(T_i^{g+}) + \Gamma_i^T \pi_i^g \qquad (20)$$

$$H(T_i^{g-}) = H(T_i^{g+}) \qquad (21)$$

$$\dot{\lambda}^T = -\frac{\partial H}{\partial \xi} \qquad (22)$$

$$\frac{\partial H}{\partial \omega} \delta\omega = 0 \;\; \forall \delta\omega \text{admiss.} \qquad (23)$$

Extremal trajectories for the $i$–th aircraft will be comprised in general of unconstrained arcs (with $D_{ij} > 0$, $\forall j \neq i$) and of constrained arcs, where the constraint is marginally satisfied ($\exists j : D_{ij} = 0$). We will accordingly distinguish the discussion of necessary conditions.

### 3.1 Unconstrained arcs

Suppose that, for the $i$–th vehicle, the separation constraints are not active in the interior of an interval $[t_i^a, t_i^b]$, $T_i^s \le t_i^a < t_i^b \le T_i^g$, i.e. $D_{ij}(t) > 0,\ j = 1, \ldots, N,\ t \in (t_i^a, t_i^b)$. The characterization of optimal solutions in the unconstrained case proceeds along the lines of the classical Dubins solution (see [13, 14, 15]). Expanding (22), one gets

$$\left[\dot\lambda_{i1}, \dot\lambda_{i2}, \dot\lambda_{i3}\right] = [0, 0, \lambda_{i,1} u_i \sin\chi_i - \lambda_{i2} u_i \cos\chi_i]\,. \tag{24}$$

By integrating (24) we obtain that conditions (19) and (20) imply that the costate components $\lambda_{i1}$ and $\lambda_{i2}$ are piecewise constant, with jumps possibly at the start and arrival time of the $i$–th vehicle. The addend in the Hamiltonian relative to the $i$–th vehicle can be written as

$$H_i = 1 + u_i \rho_i \sin(\chi_i - \psi_i) + \lambda_{i3}\omega_i,$$

where $\rho_i \stackrel{def}{=} \sqrt{\bar\lambda_{i1}^2 + \bar\lambda_{i2}^2}$ and $\psi_i \stackrel{def}{=} \operatorname{atan2}(\bar\lambda_{i2}, \bar\lambda_{i1})$. As the model is not explicitly time–dependent, we have $H_i(t) = const. \le 0$ along time–minimal unconstrained arcs. Assuming that the goal configuration always satisfies the separation constraint, it follows from (21) that $H_i(t)$ is also continuous at $t = T_i^g$.

Extremals of $H_i$ within the open segment $\{\omega_i : |\omega| < u_i/R\}$ can only obtain if

$$\frac{\partial H_i}{\partial \omega_i} = \lambda_{i3} = \bar\lambda_{i1} y_i(t) - \bar\lambda_{i2} x_i(t) + \bar\lambda_{i3} = 0. \tag{25}$$

If the condition holds on a time interval of non-zero measure, then $\dot\lambda_{i,3} = 0$ on the interval: this implies $\rho_i u_i \sin(\chi - \psi) = 0$, hence $\chi = \psi \bmod \pi$ and $\omega_i = 0$. In such an interval, the aircraft is flying on the straight route (*the supporting line*) in the horizontal $x, y$ plane described in (25). Trajectories corresponding to $\omega_i = \pm u_i/R$ correspond to circles of minimum radius $R$ followed counterclockwise or clockwise, respectively.

For each aircraft, extremal unconstrained arcs are concatenations of only two types of elementary arcs: line segments of the supporting line (denoted as "$S$"), and circular arcs of minimum radius (denoted by "$C$"). The latter type can be further distinguished between "$R$" clockwise arcs ($\omega_i = u_i/R$), and "$L$" counterclockwise arcs ($\omega_i = -u_i/R$). According to the widespread usage, subscripts will be used to denote the length of rectilinear segments, and the angular span of circular arcs.

Switchings of $\omega_i$ among $0$, $u_i/R$, and $-u_i/R$ can only occur when the aircraft center is on the supporting line. As a consequence, all extremal unconstrained paths of each vehicle are written as $C_{u_1} S_{d_1} C_{u_2} S_{d_2} \cdots S_{d_n} C_{u_n}$, with $u_i = 2k\pi$, $k$ integer, $i = 2, \ldots, n-1$.

In the case of a single vehicle, the discussion of optimal unconstrained arcs can be further refined by several geometric arguments, for which the reader is referred directly to the literature [13, 14, 15]. Optimal paths necessarily belong to either of two path types in the Dubins' sufficient family:

$$\{C_a C_b C_e\ ,\ C_u S_d C_v\} \tag{26}$$

with the restriction that

$$b \in (\pi R, 2\pi R);\ \ a, e \in [0, b],\ \ u, v \in [0, 2\pi R),\ \ d \ge 0 \tag{27}$$

A complete synthesis of optimal paths for a single Dubins vehicle is reported in [16]. The length of Dubins paths between two configurations, denoted by $L_D(\xi_i^s, \xi_i^g)$, is then unique and defines a metric on $\mathbb{R}^2 \times S^1$. One simply has $L_D(\cdot,\cdot) = R(|a| + |b| + |c|)$ for a $C_a C_b C_e$ path, and $L_D(\cdot,\cdot) = R(|u| + |v|) + d$ for a $C_u S_d C_v$ path.

In our multivehicle problem, however, other extremal paths may turn out to be optimal, and therefore have to be considered. This may happen for instance for a path of type $C_a S_b C_{2k\pi} S_e C_f$ if (and only if) the corresponding Dubins' path $C_a S_{b+e} C_f$, which is shorter, is not collision free. Arcs of type $C_{2k\pi}$ can be interpreted as waiting–in–circles maneuver for another aircraft to pass by and avoid collision (compare e.g. with current practice in conflict resolution for air traffic control). Notice explicitly that the length of two subpaths of type $\cdots C_{u_i} S_\alpha C_{2k\pi} S_\beta C_{u_{i+1}} \cdots$ and $\cdots C_{u_i} S_\gamma C_{2k\pi} S_\delta C_{u_{i+1}} \cdots$ are equivalent as far as $\alpha + \beta = \gamma + \delta$.

By "extremal trajectory" (Dubins' trajectory, respectively) we indicate henceforth a map $\mathbb{R}^+ \mapsto \mathbb{R}^2$ defined by $\left(x_i^D(t), y_i^D(t)\right)$, denoting the position of the $i$–th aircraft at time $t$ along an extremal (Dubins') path connecting $q_i^s$ to $q_i^g$.

**Remark 1**. If a set of non–colliding Dubins' trajectories exists, then this is obviously a solution of the minimum total time problem. More interestingly, if with all combinations of possible independent Dubins trajectories a collision results, then the optimal solution will contain at least a constrained arc or at least one wait circle.

**Remark 2**. Balls in the Dubins metric would be natural candidates for defining conflict envelopes. Unfortunately, they have a nontrivial geometric description, and would imply more computational load on a conflict resolution system. Probably because of this fact, along with its rather recent development, the Dubins metric has not yet been considered in practical ATM systems.

### 3.2 Constrained arcs

Some further manipulation of the cost function is instrumental to deal with constrained arcs, i.e. arcs in which at least two vehicles are exactly at the critical separation ($D_{ij} = 0,\ i \ne j$). To fix some ideas, let us consider a constrained arc involving only vehicles 1 and 2. Along a constrained arc, the derivatives of the constraint must vanish: $N = \begin{bmatrix} D_{12} \\ \dot D_{12} \end{bmatrix} = 0$, i.e.:

$$\begin{bmatrix} (x_2 - x_1)^2 + (y_2 - y_1)^2 - d^2 \\ 2(x_2 - x_1)(\dot x_2 - \dot x_1) + 2(y_2 - y_1)(\dot y_2 - \dot y_1) \end{bmatrix} = 0 \tag{28}$$

with $d = d_{12}$.

Let $\phi$ be the direction of the segment joining the two vehicles, so that

$$\begin{aligned} x_2 - x_1 &= d\cos\phi, \\ y_2 - y_1 &= d\sin\phi, \end{aligned} \tag{29}$$

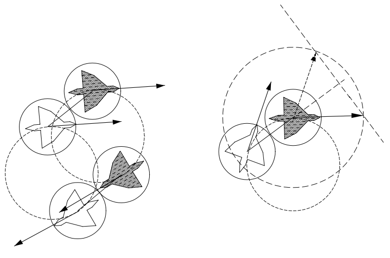


Figure 2: Possible constrained arcs for two vehicles with the same airspeed

From the second equation in (28) and using (29) one gets:

$$u_1 \cos(\phi - \chi_1) - u_2 \cos(\phi - \chi_2) = 0. \qquad (30)$$

When the constraint is active, the two aircraft envelopes are in contact, and the relative orientation of the two vehicles must satisfy (30), which defines (for given $u_1$, $u_2$) two manifolds of solutions in the space $\{(\chi_1, \chi_2, \phi) \in S^1 \times S^1 \times S^1\}$ described as

$$\begin{aligned} \mathbf{a}) \quad \chi_2^a &= \phi + \arccos\left(\frac{u_1}{u_2}\cos(\phi - \chi_1)\right); && (31) \\ \mathbf{b}) \quad \chi_2^b &= \phi - \arccos\left(\frac{u_1}{u_2}\cos(\phi - \chi_1)\right). && (32) \end{aligned}$$

The two solutions correspond to two different types (“a” and “b”) of relative configurations in contact. For instance, for $u_1 = u_2$, one has:

$$\begin{aligned} \mathbf{a}) \qquad \chi_2^a &= \chi_1; && (33) \\ \mathbf{b}) \qquad \chi_2^b &= 2\phi - \chi_1. && (34) \end{aligned}$$

In case a) the two vehicles have the same direction, while in case b) directions are symmetric with respect to the segment joining the vehicles (see fig.2). It is easy to demonstrate, [12], that the two solutions (31), (32) coincide only if $u_1 = u_2$ and

$$\phi = \chi_1 = \chi_2.$$

In order to study constrained arcs of extremal solutions, it is useful to rewrite the cost function (17) as

$$\begin{aligned} &\bar{J} = \beta^T N + \textstyle\sum_i \pi_i^s \gamma_i(\xi(T_i^s) - \xi_i^s) + \sum_i \pi_i^g \gamma_i \\ &(\xi(T_i^g) - \xi_i^g) + \textstyle\int_0^\infty \sum_i w_i + \lambda^T(\dot{\xi} - f) + \mu \ddot{D}_{12} dt, \end{aligned} \qquad (35)$$

with $\mu \geq 0$ along a constrained arc. The jump conditions at the entry point of a constrained arc, occurring at time $\tau$, are now

$$\begin{aligned} \lambda_i(\tau^-) &= \lambda_i(\tau^+) + \beta \left.\frac{\partial N}{\partial \xi}\right|_\tau && (36) \\ H(\tau^-) &= H(\tau^+) && (37) \end{aligned}$$

where $H = \sum_i w_i + \lambda^T f + \nu^T \ddot{D}_{12}$, and

$$\left(\frac{\partial N}{\partial \xi}\right)^T = 2 \begin{bmatrix} (x_1 - x_2) & u_1 \cos\chi_1 - u_2 \cos\chi_2 \\ (y_1 - y_2) & u_1 \sin\chi_1 - u_2 \sin\chi_2 \\ 0 & du_1 \sin(\phi - \chi_1) \\ (x_2 - x_1) & u_2 \cos\chi_2 - u_1 \cos\chi_1 \\ (y_2 - y_1) & u_2 \sin\chi_2 - u_1 \sin\chi_1 \\ 0 & -du_2 \sin(\phi - \chi_2) \end{bmatrix}.$$

A further distinction among constrained arcs of zero and nonzero length should be done at this point.

Consider first a constrained arc of zero length occurring at a generic contact configuration, which is completely described by the configuration of one aircraft (e.g., $\xi_c = \xi_1$), by the angle $\phi_c = \phi$, and by the contact type. Assume for the moment that there is only one constrained arc of zero length in the optimal path between start and goal of the two aircraft. Equation (36), taking into account that costates of each aircraft are determined (once the start, goal, and contact configurations are fixed) up to constants $\rho_i(\tau^-)$, $\rho_i(\tau^+)$, provides a system of 6 equations in 6 unknowns of the form

$$A(\xi_c, \phi_c) \begin{bmatrix} \rho_1(\tau^-) \\ \rho_1(\tau^+) \\ \rho_2(\tau^-) \\ \rho_2(\tau^+) \\ \beta_1 \\ \beta_2 \end{bmatrix} = 0,$$

where the explicit expression of matrix $A(\xi_c, \phi_c)$, for each contact type, can be easily evaluated in terms of $\xi_1^s$, $\xi_1^g$, $\xi_2^s$, $\xi_2^g$, and is omitted here for space limitations. Non–triviality of costates implies that $(\xi_c, \phi_c)$ must satisfy $\det(\mathbf{A}) = 0$. A further constraint on contact configurations is implied by the equality of flight times from start to contact for the airplanes, which is expressed in terms of Dubins distances as $L_D(\xi_1^s, \xi_c)/u_1 = L_D(\xi_2^s, \xi_c')/u_2$, where $\xi_c'$ denotes the configuration of aircraft 2 at contact, which is uniquely determined for each contact type. If $m$ constrained arcs of zero length are present in an optimal solution, similar conditions apply (with start and goal configurations suitably replaced by previous or successive contact configurations), yielding $2m$ equations in $4m$ unknowns.

Constrained arcs of nonzero length can be studied by recasting the problem in a reduced configuration space (see e.g. [17]). Solutions consist in optimal trajectories for aircraft that remain constantly at the minimum tolerated distance. As such, these solutions are of interest in coordinating flight of aircraft formations (employed e.g. for reducing fuel consumption by reducing aerodynamic drag). However, this type of solutions seems to be acceptable with some difficulty in commercial air traffic conflict resolution. Henceforth, we disregard the possibility that, in an optimal resolution of a conflict, there are constrained arcs of nonzero length.

# 4 Numerical computation of solutions

The necessary conditions studied in the previous sections provide useful hints in the search for an optimal solution to the problem of planning trajectories of $N$ aircraft in a common airspace. Although a complete synthesis has not been obtained so far, we will describe in this section an algorithm that finds efficient solutions to the optimal planning problem in a reasonably short time.

Based on the discussion above, the optimal conflict resolution paths for multiple aircraft may include multiple waiting circles and constrained arcs of both zero and nonzero length. Namely, we assume henceforth that

**h1** all aircraft have equal geometric characteristics and equal (constant) speed;

**h2** constrained arcs of nonzero length are not considered;

**h3** multiple zero–length constrained arcs among the same aircraft are ruled out;

**h4** the initial configurations of the aircraft are sufficiently separated.

With assumption **h4** we mean that for each aircraft, the initial configuration are collision free and guarantee that wait circles at the initial configuration are collision free (this holds for instance if the distance between the initial position of aircraft $i$ and $j$ is larger than $2\pi R\frac{\bar{u}_j}{\bar{u}_i} + 2R + \frac{d_{ij}}{2}$).

Consider first the case of two aircraft. If the Dubins' trajectories joining the way-points configurations do not collide (i.e., $D(t) \geq 0, \forall t$), this is the optimal solution. Otherwise we compute the shortest contact–free solution with wait circles at the initial configurations, and let its length be $L_f$.

Hence we look for a solution with a concatenation of two Dubins' paths and a single constrained zero–length arc of either type a) or b) for both aircraft. Such solution can be searched over a 2–dimensional submanifold of the contact configuration space ($\mathbb{R}^2 \times S^1 \times S^1$). The optimal solution can be obtained by using any of several available numerical constrained optimization routines: computation is sped up considerably by using very efficient algorithms made available for evaluating Dubins' paths ([16]). The lenght $L_c$ of such solution is compared with $L_f$, and the shorter solution is retained as the two–aircraft optimal conflict management path with at most a single constrained zero-length arc (OCMP21, for short). Some examples of OCMP21 solutions are reported in Figure 3.

These solutions refer to a scenario with two equal aircraft, with mass $m = 185$klbm, airspeed $V_{max} = 340$ft/sec, load factor $n = 0.9g$, max. bank angle $\varphi_{max} = 20$deg., lift constant $\beta_L = 4800$lb/ft, hence (for $\gamma = 0$), the minimum curvature radius results $R = 2.4$n. miles.

If $N$ aircraft fly in a shared airspace, their possible conflicts can be managed with the following multilevel policy:

**Level 0** Consider the unconstrained Dubins paths of all aircraft, which may be regarded as $N$ single–aircraft, optimal conflict management paths, or OCMP10. If no collision occurs, the global optimum is achieved, and the algorithm stops. Otherwise compute the shortest contact–free paths (with wait circles) and go to next level;

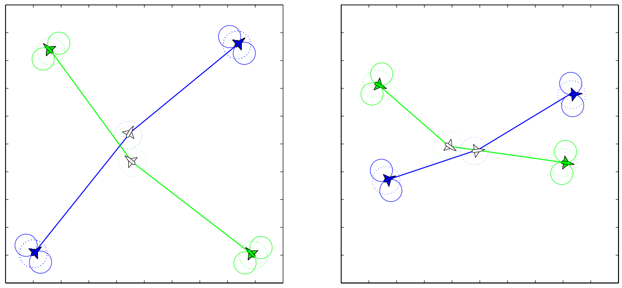

Figure 3: Numerically computed solutions to optimal cooperative conflict resolution for two aircraft. Minimum curvature circles are reported at the start and goal configurations, along with safety discs of radius $d/2$ (dashed). Optimal solutions consist of two unconstrained Dubins' trajectories for each aircraft, pieced together with a zero–length constrained arc.

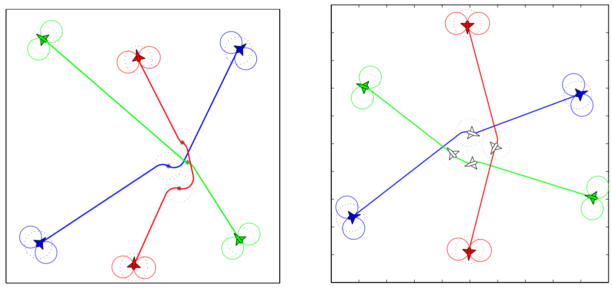

Figure 4: Two cases of three–aircraft conflict resolution. Left: a level 2 solution whereby the aircraft starting in the middle contacts first the one arriving on its right, and after the one arriving from left. Right: a level 2 resolution that generates a roundabout–like maneuver.

**Level 1** Consider the $M = 2\binom{N}{2}$ possible solutions with a single contact (of either type a or b), between two aircraft, and possibly wait circles for other aircraft, and compute the shortest path in this class. If this is longer than the shortest path obtained at level 0, exit. Otherwise, continue;

**Level $m \geq 2$.** Consider the $M\prod_{\ell=1}^{m-1}(M - 2^\ell)$ possible solutions involving $m$ zero–length constrained arcs between different pairs of aircraft and (possibly) wait circles for other aircraft, and compute the shortest path in this class. If this is longer than the shortest path obtained at level $m - 1$, exit. Otherwise, continue;

A few three–aircraft conflict resolution trajectories at different levels are reported in Figure 4. When the number of aircraft increases, the number of optimization problems to be solved grows combinatorially. However, in practice, it is hardly to be expected that conflicts between more than a few vehicles at a time have to be managed, that require solutions of level higher than 2.

# 5 Conclusion

In this paper, we have studied the problem of planning trajectories of multiple Dubins' vehicles in a plane. Necessary conditions have been derived, and an algorithm for numerically finding solutions has been described.

Future work on this topic will address the problem of finding a complete optimal synthesis at least for the simplest cases ($N = 2$), and extending to the case of variable longitudinal velocity. Further refinement of the algorithm will be sought, that could exploit more of the rich structure optimal solutions must satisfy.

# References


[1] Honeywell Inc., "Markets Report," *Tech. rep. NASA Contract AATT*, 1996.

[2] T. S. Perry, "In search of the future of air traffic control," *IEEE Spectrum*, Vol. 34, pp. 18-35, August 1997.

[3] RTCA Task Force 3, "Final Tech. Rep.: Free Flight Implementation," *Radio Technical Commission for Aeronautics*, October 1995.

[4] Ed. Board, "Special Report on Free Flight," *Aviation Week and Space Technology*, July 1995.

[5] C. Tomlin, G. Pappas, J. Kosecka, J. Lygeros and S. Sastry, "Advanced air traffic automation: a case study in distributed decentralized control," *Control Problems in Robotics and Automation, ed. B. Siciliano and K. Valavanis, Springer-Verlag*, pp. 261-295, 1997.

[6] R. C. Nelson, *Flight Stability and Automatic Control*, McGraw-Hill, 1989.

[7] B. Etkin, *Dynamics of Atmospheric Flight*, Wiley, 1982.

[8] C. Tomlin, G. J. Pappas and S. Sastry, "Conflict Resolution for Air Traffic Management: A Case Study in Multi-Agent Hybrid Systems," *TAC*, Vol. 43, N. 4, pp. 509-521, April 1998.

[9] P. K. Menon, G. D. Sweriduk and B. Sridhar, "Optimal Strategies for Free-Flight Air Traffic Conflict resolution," *Journ. of Guidance, Control, and Dynamics*, Vol. 22, N. 2, pp. 202-211, March-April 1999.

[10] G. Meyer, R. Su and L. R. Hunt, "Application of nonlinear transformations to automatic flight control," *Automatica*, Vol. 20, pp. 103-107, 1984.

[11] H. Erzberger and W. Nedell, "Design of Automated System for management of arrival traffic," *NASA*, TM 102201, June 1989.

[12] A. Bicchi and L. Pallottino, "Optimal Cooperative Conflict Resolution for Air Traffic Management Systems," subm. *IEEE Trans. on Intelligent Transportation Systems*, 2001.

[13] L. E. Dubins, "On curves of minimal length with a constraint on average curvature and with prescribed initial and terminal positions and tangentIEEE Trans. on Intelligent Transportation Systems," *American Journal of Mathematics* , Vol. 79, pp. 497-516, 1957.

[14] H. J. Sussmann and G. Tang, "Shortest Paths for the Reeds–Shepp Car: a Worked Out Example of the Use of Geometric Techniques in Nonlinear Optimal Control," *SYCON*, N. 91-10, 1991.

[15] J.D. Boissonnat, A. Cerezo and J. Leblond, "Shortest Paths of Bounded Curvature in the Plane," *IEEE ICRA*, pp. 2315-2320, 1992.

[16] X.N. Bui, P. Souères, J-D. Boissonnat and J-P. Laumond, "Shortest path synthesis for Dubins non–holonomic robots," *IEEE ICRA*, pp. 2-7, 1994.

[17] A. Bicchi and L. Pallottino, "Optimal planning for coordinated vehicles with bounded curvature," subm. *Proc. Int. Work. Algorithmic Foundations of Robotics*, ed. B. Donald and K. Lynch and D. Rus, March 2000.